



Algorithmized Modelling, Simulation and Validation of Clearness Index in Four Regions of Uganda

Mundu, Mustafa Muhamad^a, Nnamchi, Stephen Ndubuisi^b, and Ukagwu, Kelechi John^c

- Department of Physical Sciences, SEAS, Kampala International University, P.O. Box 20000, Kampala, Uganda, mundu.mustafa@kiu.ac.ug, ORCID; 0000-0003-1345-9999.*
- Department of Mechanical Engineering, SEAS, Kampala International University, P.O. Box 20000, Kampala, Uganda, stephen.nnamchi@kiu.ac.ug, ORCID; 0000-0002-6368-2913.*
- Department of Electrical, Telecommunication and Computer Engineering, SEAS, Kampala International University, P.O. Box 20000, Kampala, Uganda, ukagwu.john@kiu.ac.ug, ORCID; 0000-0002-9604-4598.*

Abstract

Uganda as a developing nation, needs to exploit her renewable energy potential to maximum through extensive research in the field of solar engineering. Thus, this work tries to build up a comprehensive clearness index model at three categories; national, regional and district on periodic (monthly) and non-periodic (yearly) basis for this purpose. Approximately, this quest is proceeded with the acquisition of quadragenarious data from both National Aeronautics and Space Administration (NASA) and the on-station data from four locations in Uganda. The data were arranged in the structural order of the proposed clearness index (CI) model in the MS-Excel spread sheet and later exported to OriginLab to obtain the coefficients of the CI models. The statistical inference; the coefficient of determination (R^2), were all tending to unity (1) which indicates the strength of the models obtained. It is observed that clearness index ranges for the different regions of Uganda: Northern (0.5288 – 0.6077), Eastern (0.5609 – 0.6077), Central (0.5123 – 0.6224) and Western (0.5123 – 0.5893). Besides, the empirical validation of the model results with the on-station data was carried out. There was good agreement between the simulated and on-station data with the trace of deviations which could be attributed to the impact of latitude and longitude of the failed locations. Furthermore, the present models were compared with the existing models, the deviation between the measured and the present model was insignificant compared to the existing models. Therefore, the present model could be employed in the advancement of solar technologies in Uganda.

Keywords: Modelling, Simulation, Algorithm, Validation, Clearness index and Uganda

1. Introduction

Past literature (research) studies of clearness or cloudiness index is based on regressional or non-regressional (differential) models. The regressional models are built on mathematical functions (linear,

quadratic, cubic, exponential, logarithmic functions) whereas; the differential models are intrinsically defined by any of the mathematical functions. The models are expressed by the following physical indicators; sunshine hours, average sunshine hours,

*Corresponding author, Department of Physical Sciences, KIU, Kampala, Uganda
Email address: mundu.mustafa@kiu.ac.ug, +256773247249

relative sunshine hours, average relative sunshine hours, latitude, temperature difference, average temperature, humidity, relative humidity and humidity difference. Some researchers in different locations have attempted to combine the indicators to generate clearness index for their respective locality [1], [2], [3], [4], [5], [6], [7]. Also, improvement in the clearness index was sought through applications of different mathematical functions and their combinations to develop clearness index models. It has been of the state-of-the-art that these models be validated; many researchers have resorted to use of statistical tools as means of validating their models [8], [9], [10] and [11]. The common statistical tools employed for analytical validation are; coefficient of determination (R^2), correlation coefficient (r), mean percentage error (MPE), relative root mean square error (RRMSE), root mean square error (RMSE), global performance indicator (GPI), mean bias error (MBE) but as R^2 is the approaching unity and vice versa, indicates that there is minimal error or good agreement between the measured and simulated (modeled) data. Ultimately, on this basis of minimal error, the model for clearness index is implemented. Conversely, when the statistical tool (R^2) are tending to zero, imply that there is significant error or deviation between the measured and model simulated data thus the model has to be refined (improved on by adding more function and more order and vice versa) or otherwise discarded. Nowadays, most researchers are not satisfied with statistical tools alone, they implement visual validation (empirical validation) whereby the measured and the simulated data are interpolated and visualized for fitness (agreement). The relevant models consulted are built on single function, bi-function, triple function quadra-function penta-function.

Systematically, the single indicator models in the likes of Nwokolo and Otse [8] emphasized on analytical (statistical) approach as a means of validating two year solar models using statistical indicators of; MBE, MPE, RMSE, RRMSE, R^2 , and GPI. However, the present work will validate solar models on empirical basis in addition to statistical

approach (to portray the agreement between the measured and simulated data) for the purposes of authenticating the validity of the developed solar models. Retrospectively, Yusuf [9] developed and validated clearness index model based on only relative sunshine hour (rsh) in Iseyin in western Nigeria with good MBE, the absolute MBE and RMSE. However, the model is not comprehensive compared to Rijks and Huxley [12], and Mubiru *et al.* [13] who developed multiple independent variables. Similarly, the present work will engage more sensitive variables (latitude, ϕ , and *rsh*) to develop flexible clearness index model for Uganda. Also the model will be subjected to practical validation to substantiate its accuracy. Beyond trending of experimental data, the present work will embark on comprehensive model construction for the necessary solar models needed for design applications of solar thermal and photovoltaic systems in Uganda. Conversely, Asilevi *et al.* [14] proposed fourth order differential model (modified bi-harmonic) for mathematical description of solar parameters (sunshine hour for Ghana) without proffering its solution, instead of applying popular regressional models (non-differential) in developing mathematical relationship between solar parameters. However, the present work will employ higher order regressional model; which accounts for variation in periods and the interaction between independent variables.

Correspondingly, Assi *et al.* [15], have developed and validated linear global solar radiation model using rsh for United Arab Emirates. The present study will use both statistical and non-statistical approaches in assessing the validity of the models to ascertain the deviation between the measured and estimated variables. Equally, Ahwide and El-Kafrawy [16] obtained horizontal daily solar sunshine duration data in Libya but the present work will use more normalized variable; relative sunshine hour which takes into account the daylength.

Moreover, a number of models for global solar radiation estimation have been developed using clearness index and relative sunshine hours [6], [7], [5], [4], [3], [1] and [2]. Similarly, the present work will use latitude of location to specify every single

point of interest in developing similar models for Uganda.

Furthermore, Muzathik *et al.* [17] tested existing extensive models using statistical error analysis in Malaysia. The present work will back up their tests with empirical and visual tests of models. Further, Matuszko [18] developed the link between sunshine and cloudiness using quadratic regression and found that *rsh* is commensurate to clearness index. But the present work will extend to third order model.

However, Zhu *et al.* [19] measured sunshine hours using the method of total cloud amount (CTA) to validate existing models in China. The present work will develop and test the validity of the present models and possibly the existing models in Uganda. Alam *et al.* [20], developed solar models using three parameters; cloudiness index, temperature difference, ΔT and sunshine hours on empirical data for Pakistan. For the similar work in Uganda, the present work has substituted temperature difference with latitude (ϕ) which is more sensitive to change in solar parameters; clearness index (K_T), relative sunshine hours (*rsh*) and sunshine hours (*sh*). Their solar model is outstanding for using temperature to substitute relative sunshine hours in literature models. However, K_T , is not sensitive to temperature difference compared to relative sunshine hours which is physical and practical variable for indicating K_T . Conversely to the present work, Mohandes and Rehman [21] proposed machine learning algorithms for estimating sunshine duration in Saudi Arabia. The literature review has been Algorithmized or demystified in Figure 1 below.

This paper will; establish a workable or feasible model for predicting clearness index in Uganda, simulate both present and existing models in order to test their validity, and present validated clearness index models for future estimation of global solar radiation in Uganda. These objectives are to be realized on logical steps or algorithm from modelling to validation of the entire process; materials and method, presentation of results and discussion of results, conclusions and recommendations subsequently.

High lighting the gaps found in the literature; all the models are non-periodic (not dependent on time); the indicators are not combined; the order is limited to four. But however, the present work will certainly fill these gaps by presenting more robust flexible model; combined, fifth order and time dependent model in modeling clear index within the confine of Uganda for application in solar technologies (helio-photovoltaic and helio-thermal systems) within the country to boost green power generation for present and future generation.

2. Materials and Methods

In the algorithm (Figure. 2 below), the method starts with introduction, data acquisition, offset data queries including data filtering, data management, model development, graphical representation of data, testing of model and it ends with implementation of finding. Subsequent to literature survey, the process of data acquisition started with collecting the secondary data from NASA POWER (Prediction of Worldwide Energy Resources), a source for surface meteorology and solar energy. The meteorological data collected for this study focused on approximately forty year climatological or quadragenarian data from 1984 to 2018, on sunshine hours duration, relative sunshine hours, wind speed and clearness index for all the 122 districts (as of 2017/2018) of the four regions of Uganda (Lat. $1^{\circ} 22' 14.63''$ N, Long. $32^{\circ} 18' 11.67''$ E); the Northern region (32 districts), Eastern region (34 district), Central region (25 district) and Western region (31 districts). In addition, the other sources of secondary data were AccuWeather (for weather forecasts), and HOMER meteorological centers. Measurements of radiation data were collected from four sites throughout the country. Each location in the district represents a region. The measurements were done using pyrometers installed at four different locations.

A location in Lira district representing the district

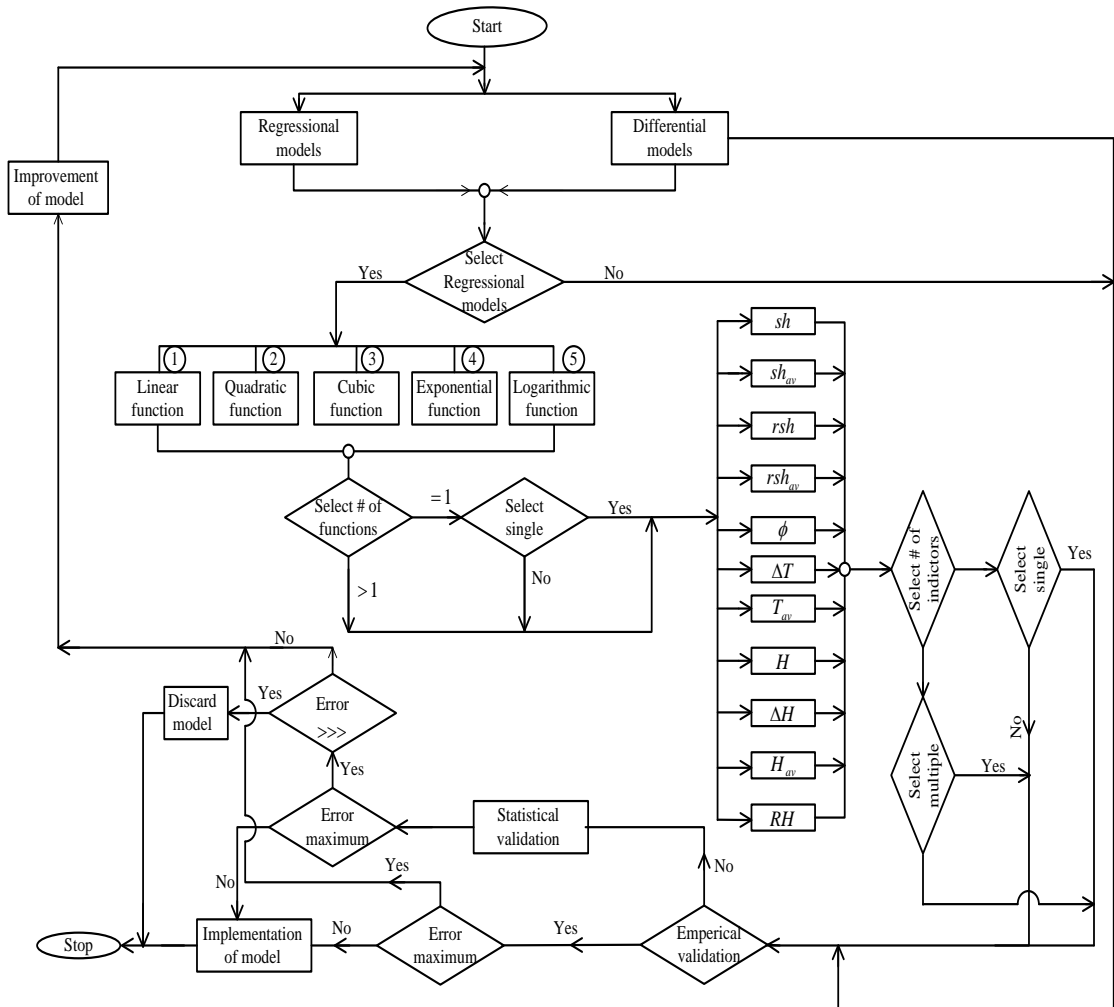


Figure 1. An algorithm for literature survey

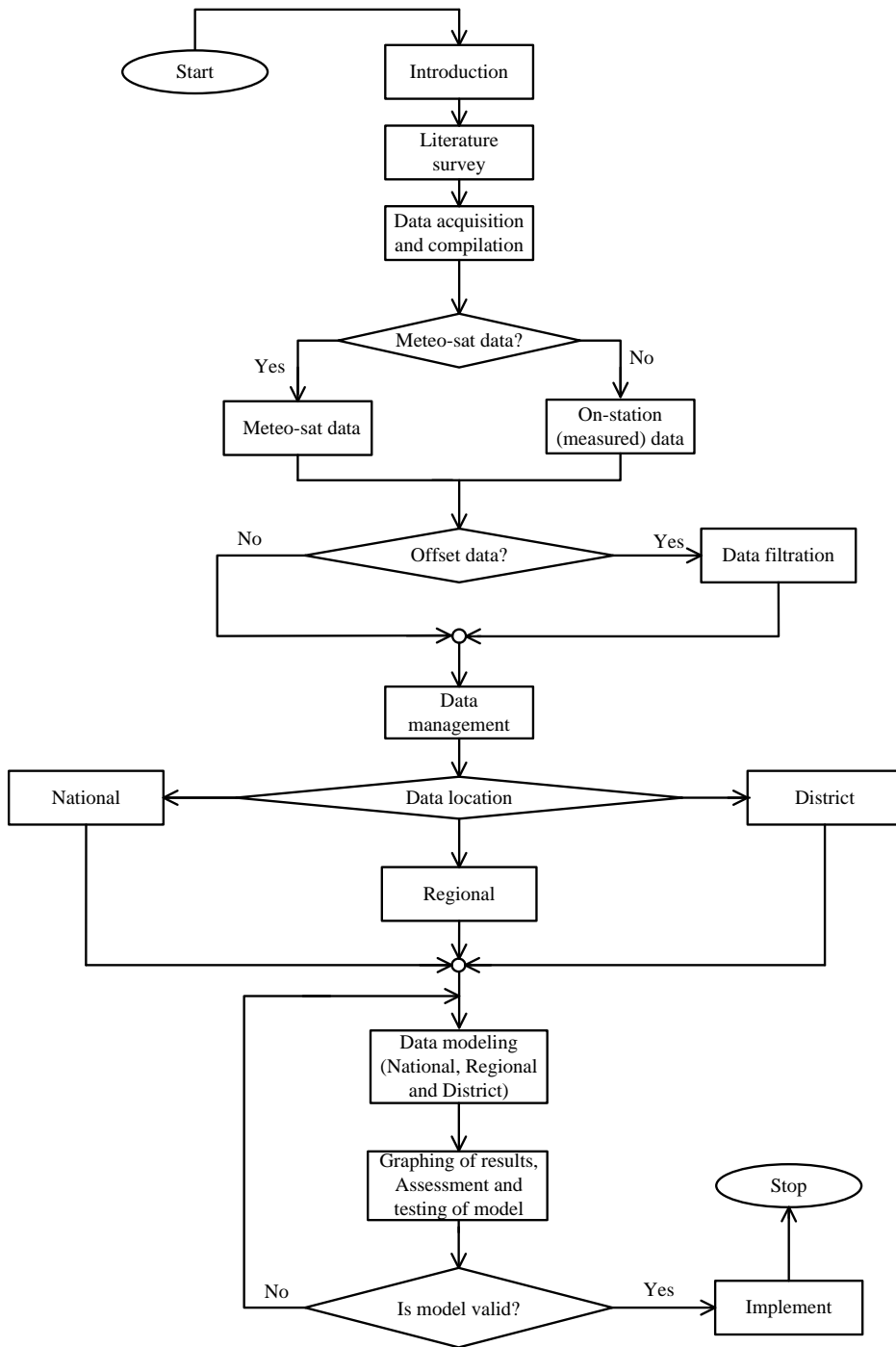


Figure 2. An algorithm for data acquisition and processing

(Lat. 02° 17' N, Long. 32° 57' E) for Northern region, another in Tororo district representing the district (Lat. 0° 45' N, Long. 34° 12' E) for Eastern region, for Kampala district (Lat. 00°20' N, Long. 32°30' E) representing the Central region, the location is at Makerere University, Department of Physics (Lat. 00° 19' N, Long. 32° 40' E). While, the location in Mbarara district (Lat. 0° 35' S, Long. 60° 40' E) represents the Western region. However, some of the measured data obtained from the different stations were inconsistent that were outside the expected range of values. This could possibly be due to calibration issues related to the instruments and that it is recommended that a re-calibration be done to the affected instruments. In the appropriate layout of the present study (at national, regional and district levels), the data sets were processed accordingly. The latitude (ϕ), the number of days (n) and declination (δ) were used to compute the daylength in a particular location. The data set were filtered using Microsoft Excel by removing insolation values in early morning and late evening hours, the concentration was from 9:00 am to 5:00 pm.

2.1 Clearness Index Models

The present model (periodic or monthly) is expressed in Equation (1)

$$k_{T,i} = b_{0,i} + b_{1,i} \cos \phi_i + b_{2,i} rsh_i + b_{3,i} rsh_i \cos \phi_i + b_{4,i} \cos^2 \phi_i + b_{5,i} rsh_i^2 + b_{6,i} rsh_i \cos^2 \phi_i + b_{7,i} rsh_i^2 \cos \phi_i + b_{8,i} \cos^3 \phi_i + b_{9,i} rsh_i^3 \quad (-) \quad (1)$$

$i \in \{ \text{January, February, March, April, May, June, July, August, September, October, November, December} \}$

where; $b_0, b_1, b_2, b_3, b_4, b_5, b_6, b_7, b_8$ and b_9 are constants determined based on the location of a place.

Commensurately, this work presents non-periodic clearness index model for Kampala (Central region.) as shown in Equation (2)

$$k_{T,i} = b_{0,i} + b_{1,i} \cos \phi_i + b_{2,i} rsh_i + b_{3,i} rsh_i \cos \phi_i + b_{4,i} \cos^2 \phi_i + b_{5,i} rsh_i^2 + b_{6,i} rsh_i \cos^2 \phi_i + b_{7,i} rsh_i^2 \cos \phi_i + b_{8,i} \cos^3 \phi_i + b_{9,i} rsh_i^3 \quad (-) \quad (2)$$

Rijks and Huxley [12] presented a maiden clearness index model for Uganda (Western region) in equation (3)

$$k_T = \frac{\bar{H}}{\bar{H}_0} = 0.24 + 0.47 \frac{n}{N} \quad (3)$$

Also, Mubiru et al. [13] correlated a clearness index model for Kampala district (Central Uganda) in Equation (4)

$$k_T = \frac{\bar{H}}{\bar{H}_0} = 0.288 + 0.154 \left(\frac{n}{N} \right) + 0.448 \left(\frac{n}{N} \right)^2 \quad (4)$$

where rsh is equivalent to $\frac{n}{N}$ in Equations (3) and

(4).

3.0 Results and Discussion

This section is devoted for the presentation of tables and figures accruing from the results. Subsequently, the discussion of the tables and figures from the results.

3.1 Results

Tables 1-7 below contain clearness index models for national (Table 1), regional (Tables 2-5), sample representative of districts (Tables 6-7); where the first twelve rows in each table is clearness index model for months (periods); January to December respectively, in Tables 1-7. The model is formulated on periodic to cater for monthly or periodic change in time and non-periodic, which is independent of time. The models were formulated for different categories; non-regional (national), regional (north, east, central and west), selected districts (Tororo and Mbarara) in order to establish specific and accurate model for each category. All the models from Tables 1-7 were developed from quadragenarious satellite data (NASA), after filtration and prearrangement and programming (to suit the proposed model structure in Equations 1 and 2) in Microsoft Excel spreadsheet, the data were exported to OriginLab to generate the coefficients of the models and coefficient of determination (R^2), for statistical inference on the models (which is a measure of deviation from the true mean). However, the suitability of each category will be revealed once validated with the measured data. The validity of Tables 1-7 above is shown using statistical tool (R^2)

while the empirical validity of the models will be carried out in the subsequent section.

The table of results are accompanied by Figures 1-5 as shown below. Figure 1 depicts periodic (monthly; (a). January to (l). December) validation of clearness index based on Tororo district meteorological measured data. Correspondingly, Figure 2 contains non-periodic validation of clearness index based on Tororo district meteorological measured data.

Similarly, Figure 3 shows periodic (monthly; (a). January to (i). December) validation of clearness index based on Mbarara district meteorological measured data. Correspondingly, Figure 4 comprises the non-periodic validation of clearness index based on Mbarara district meteorological measured data. Lastly, Figure 5 gives a comparative picture of present work and existing clearness index models in Uganda.

3.2 Discussions

Considering Table 1, the coefficient of determination (R^2) for periodic models range (0.9959 to 1.0000) whereas that of non-periodic model is 0.7922 which implies that the periodic models are superior to the non-periodic model, because the periodic models are based on monthly data whereas the non-period is annual data. The monthly models appears to be more accurate than the non-periodic (yearly) because of negligible perturbation in the weather condition that occur during a month compared to appreciable perturbations during the year (sequel to seasonal changes).

In view of Table 2, the coefficient of determination (R^2) for periodic models range (0.9999 to 1.0000) whereas that of non-periodic model is 0.9952 which implies that the periodic models are higher to the non-periodic model, since the periodic models are based on monthly data whereas the non-period is annual data. The monthly models appears to be more accurate than the non-periodic (yearly) could be attributed to insignificant fluctuation in the weather condition that occur during a month as compared to significant variation during the year (sequel to seasonal changes).

Similarly, Table 3 contains the coefficient of determination (R^2) for periodic clearness index models (1.0000) whereas that of non-periodic model is 0.9627 which implies that the periodic models are superior to the non-periodic model, however, the annual data did not experience so much variation due to closeness of R^2 .

Likewise, Tables 4 (and 5) reports the coefficient of determination (R^2) for periodic models range (0.9999 to 1.0000) whereas that of non-periodic model is 0.9988 (0.9996) which implies that the periodic models are slightly superior to the non-periodic model as indicated by the R^2 value. This implies that the region was not readily susceptible or experience mild change in weather conditions. Thus, the region was buffered to the fluctuations in weather conditions.

Comparing Tables 1 to 5, the strength of the clearness index models developed is as follows; In Tables 6 (and 7) depicted highest coefficient of determination for periodic (1.0000) and non-periodic (1.0000) which implies that the model data were stable invariably, thus the stability of their corresponding models.

Therefore, tables 6 and 7 appear to be more robust than table 1 to 5 since they are built on mono latitude whereas the others were developed on multiple latitudes, latitude is one of the sensitive indicators upon which the clearness index model were developed upon. Besides, the statistical inferential tool (R^2), Figures 1 – 5 vividly portrays the agreement (validity) between the measured and the model simulated results.

Virtually, Figures 1 (a- i) support the high value of R^2 as presented in Tables 1 – 7 with exception of Figure 1 (e) representing Tororo district in the month of May. Also, Mbarara district witnessed similar deviation but in the month of November (Figure 3 (k)).

Table 1. National (periodic and non-periodic) models

S#	Model	R^2 (COD)	Model type
1.	$k_{T, Jan} = -5.90 \times 10^{-3} + 1.77 \times 10^4 \cos \phi + 69.8 rsh - 2.16 \times 10^2 rsh \cos \phi - 1.76 \times 10^4 \cos^2 \phi + 55.4 rsh^2 + 1.47 \times 10^2 rsh \cos^2 \phi - 55.5 rsh^2 \cos \phi + 5.84 \times 10^3 \cos^3 \phi + 1.87 \times 10^{-2} rsh^3$ (-)	0.9997	Periodic (monthly) models
2.	$k_{T, Feb} = -1.38 \times 10^5 + 4.15 \times 10^5 \cos \phi + 1.31 \times 10^2 rsh - 2.58 \times 10^2 rsh \cos \phi - 4.16 \times 10^5 \cos^2 \phi - 2.07 rsh^2 + 1.28 \times 10^2 rsh \cos^2 \phi + 2.02 rsh^2 \cos \phi + 1.39 \times 10^5 \cos^3 \phi + 2.85 \times 10^{-2} rsh^3$ (-)	0.9997	
3.	$k_{T, Mar} = 0.01676 + 0.22008 \cos \phi + 0.52044 rsh - 8.81 \times 10^{-3} rsh \cos \phi + 0.05097 \cos^2 \phi - 7.12 \times 10^{-7} rsh^2 + 4.41 \times 10^{-4} rsh \cos^2 \phi + 7.10 \times 10^{-7} rsh^2 \cos \phi - 0.01711 \cos^3 \phi + 1.23 \times 10^{-9} rsh^3$ (-)	1.0000	
4.	$k_{T, Apr} = 1.13 \times 10^5 - 3.41 \times 10^5 \cos \phi + 1.11 \times 10^3 rsh - 2.23 \times 10^3 rsh \cos \phi + 3.42 \times 10^5 \cos^2 \phi + 0.628 rsh^2 + 1.11 \times 10^3 rsh \cos^2 \phi - 7.03 \times 10^{-1} rsh^2 \cos \phi - 1.14 \times 10^5 \cos^3 \phi + 4.44 \times 10^{-2} rsh^3$ (-)	0.9997	
5.	$k_{T, May} = 2.16 \times 10^{-02} + 0.206 \cos \phi + 0.52004 rsh - 8.56 \times 10^{-05} rsh \cos \phi + 6.49 \times 10^{-02} \cos^2 \phi - 1.93 \times 10^{-06} rsh^2 + 4.17 \times 10^{-05} rsh \cos^2 \phi + 1.93 \times 10^{-06} rsh^2 \cos \phi - 2.17 \times 10^{-02} \cos^3 \phi - 4.67 \times 10^{-11} rsh^3$ (-)	0.9997	
6.	$k_{T, Jun} = 2.41 \times 10^{-2} + 0.198 \cos \phi + 0.51961 rsh + 7.84 \times 10^{-4} rsh \cos \phi + 7.22 \times 10^{-2} \cos^2 \phi + 2.04 \times 10^{-7} rsh^2 - 3.92 \times 10^{-04} rsh \cos^2 \phi - 2.04 \times 10^{-07} rsh^2 \cos \phi - 2.40 \times 10^{-02} \cos^3 \phi - 1.81 \times 10^{-13} rsh^3$ (-)	0.9959	
7.	$k_{T, Jul} = 1.97 \times 10^{-2} + 0.212 \cos \phi + 0.52 rsh + 7.52 \times 10^{-4} rsh \cos \phi + 5.89 \times 10^{-2} \cos^2 \phi + 5.13 \times 10^{-6} rsh^2 - 3.73 \times 10^{-4} rsh \cos^2 \phi - 5.17 \times 10^{-6} rsh^2 \cos \phi - 1.96 \times 10^{-2} \cos^3 \phi + 2.62 \times 10^{-8} rsh^3$ (-)	1.0000	
8.	$k_{T, Aug} = 2.65 \times 10^{-2} + 0.191 \cos \phi + 0.51948 rsh + 1.03 \times 10^{-3} rsh \cos \phi + 7.93 \times 10^{-2} \cos^2 \phi + 6.60 \times 10^{-6} rsh^2 - 5.10 \times 10^{-4} rsh \cos^2 \phi - 6.65 \times 10^{-6} rsh^2 \cos \phi - 2.64 \times 10^{-2} \cos^3 \phi + 2.77 \times 10^{-8} rsh^3$ (-)	1.0000	
9.	$k_{T, Sep} = 2.64 \times 10^{-2} + 0.192 \cos \phi + 0.51947 rsh + 1.06 \times 10^{-3} rsh \cos \phi + 7.88 \times 10^{-2} \cos^2 \phi + 2.82 \times 10^{-6} rsh^2 - 5.27 \times 10^{-4} rsh \cos^2 \phi - 2.82 \times 10^{-6} rsh^2 \cos \phi - 2.62 \times 10^{-2} \cos^3 \phi + 8.27 \times 10^{-15} rsh^3$ (-)	0.9972	
10.	$k_{T, Oct} = 2.75 \times 10^{-2} + 0.188 \cos \phi + 0.51961 rsh + 7.83 \times 10^{-4} rsh \cos \phi + 8.21 \times 10^{-2} \cos^2 \phi + 4.08 \times 10^{-6} rsh^2 - 3.89 \times 10^{-04} rsh \cos^2 \phi - 4.08 \times 10^{-06} rsh^2 \cos \phi - 2.73 \times 10^{-02} \cos^3 \phi - 7.93 \times 10^{-14} rsh^3$ (-)	0.9999	
11.	$k_{T, Nov} = 1.50 \times 10^5 - 4.53 \times 10^5 \cos \phi + 5.12 \times 10^3 rsh - 1.03 \times 10^4 rsh \cos \phi + 4.56 \times 10^5 \cos^2 \phi + 28.6 rsh^2 + 5.16 \times 10^{03} rsh \cos^2 \phi - 28.6 rsh^2 \cos \phi - 1.53 \times 10^{05} \cos^3 \phi - 4.48 \times 10^{-02} rsh^3$ (-)	0.9995	
12.	$k_{T, Dec} = 1.02 \times 10^{-2} + 0.240 \cos \phi + 0.52043 rsh - 8.61 \times 10^{-4} rsh \cos \phi + 3.13 \times 10^{-2} \cos^2 \phi - 1.02 \times 10^{-6} rsh^2 + 4.30 \times 10^{-04} rsh \cos^2 \phi + 1.02 \times 10^{-06} rsh^2 \cos \phi - 1.05 \times 10^{-02} \cos^3 \phi - 4.61 \times 10^{-15} rsh^3$ (-)	1.0000	
13.	$k_{T, np} = -8.85 \times 10^{-3} + 0.297 \cos \phi + 0.521 rsh - 1.87 \times 10^{-3} rsh \cos \phi - 2.52 \times 10^{-2} \cos^2 \phi - 9.14 \times 10^{-7} rsh^2 + 9.33 \times 10^{-4} rsh \cos^2 \phi + 9.14 \times 10^{-7} rsh^2 \cos \phi + 8.17 \times 10^{-3} \cos^3 \phi - 1.18 \times 10^{-12} rsh^3$ (-)	0.7922	

Table 2. Northern Region (periodic and non-periodic) models

S#	Model	R^2 (COD)	Model type
1.	$k_{T, Jan} = 44.6 - 1.07 \cos \phi + 0.523rsh - 5.99 \times 10^{-3} rsh \cos \phi + 1.35 \cos^2 \phi - 5.81 \times 10^{-8} rsh^2$ $+ 3.00 \times 10^{-3} rsh \cos^2 \phi + 6.49 \times 10^{-7} rsh^2 \cos \phi - 0.45 \cos^3 \phi - 2.85 \times 10^{-7} rsh^3$ (-)	1.0000	Periodic (monthly) models
2.	$k_{T, Feb} = 0.546 - 1.37 \cos \phi + 0.52rsh + 1.15 \times 10^{-4} rsh \cos \phi + 1.64 \cos^2 \phi + 5.05 \times 10^{-6} rsh^2$ $- 5.48 \times 10^{-5} rsh \cos^2 \phi - 5.10 \times 10^{-6} rsh^2 \cos \phi - 0.548 \cos^3 \phi + 2.27 \times 10^{-8} rsh^3$ (-)	1.0000	
3.	$k_{T, Mar} = 0.55 - 1.38 \cos \phi + 0.520rsh - 5.19 \times 10^{-4} rsh \cos \phi + 1.66 \cos^2 \phi + 6.26 \times 10^{-6} rsh^2$ $+ 2.63 \times 10^{-4} rsh \cos^2 \phi - 6.31 \times 10^{-6} rsh^2 \cos \phi - 0.553 \cos^3 \phi + 2.29 \times 10^{-8} rsh^3$ (-)	1.0000	
4.	$k_{T, Apr} = 0.482 - 1.18 \cos \phi + 0.521rsh - 1.84 \times 10^{-3} rsh \cos \phi + 1.45 \cos^2 \phi - 5.15 \times 10^{-6} rsh^2$ $+ 9.17 \times 10^{-4} rsh \cos^2 \phi + 5.14 \times 10^{-6} rsh^2 \cos \phi - 0.485 \cos^3 \phi + 4.92 \times 10^{-9} rsh^3$ (-)	1.0000	
5.	$k_{T, May} = 0.584 - 1.4 \cos \phi + 0.519rsh + 1.22 \times 10^{-3} rsh \cos \phi + 1.76 \cos^2 \phi + 9.13 \times 10^{-6} rsh^2$ $- 6.04 \times 10^{-4} rsh \cos^2 \phi - 9.22 \times 10^{-6} rsh^2 \cos \phi - 0.586 \cos^3 \phi + 4.51 \times 10^{-8} rsh^3$ (-)	1.0000	
6.	$k_{T, Jun} = 0.623 - 1.60 \cos \phi + 0.518rsh + 3.99 \times 10^{-3} rsh \cos \phi + 1.87 \cos^2 \phi + 1.93 \times 10^{-5} rsh^2$ $- 1.99 \times 10^{-3} rsh \cos^2 \phi - 1.94 \times 10^{-5} rsh^2 \cos \phi - 0.624 \cos^3 \phi + 1.06 \times 10^{-7} rsh^3$ (-)	1.0000	
7.	$k_{T, Jul} = 0.614 - 1.57 \cos \phi + 0.518rsh + 3.08 \times 10^{-3} rsh \cos \phi + 1.84 \cos^2 \phi + 2.48 \times 10^{-5} rsh^2$ $- 1.53 \times 10^{-3} rsh \cos^2 \phi - 2.51 \times 10^{-5} rsh^2 \cos \phi - 0.615 \cos^3 \phi + 1.41 \times 10^{-7} rsh^3$ (-)	1.0000	
8.	$k_{T, Aug} = 0.626 - 1.61 \cos \phi + 0.519rsh + 1.37 \times 10^{-3} rsh \cos \phi + 1.88 \cos^2 \phi + 2.34 \times 10^{-5} rsh^2$ $- 6.75 \times 10^{-4} rsh \cos^2 \phi - 2.36 \times 10^{-5} rsh^2 \cos \phi - 0.628 \cos^3 \phi + 1.01 \times 10^{-7} rsh^3$ (-)	1.0000	
9.	$k_{T, Sep} = 0.661 - 1.71 \cos \phi + 0.519rsh + 2.10 \times 10^{-3} rsh \cos \phi + 1.99 \cos^2 \phi + 1.12 \times 10^{-5} rsh^2$ $- 1.04 \times 10^{-3} rsh \cos^2 \phi - 1.13 \times 10^{-5} rsh^2 \cos \phi - 0.663 \cos^3 \phi + 5.42 \times 10^{-8} rsh^3$ (-)	1.0000	
10.	$k_{T, Oct} = 0.675 - 1.76 \cos \phi + 0.52rsh + 8.31 \times 10^{-4} rsh \cos \phi + 2.03 \cos^2 \phi + 2.03 \times 10^{-5} rsh^2$ $- 4.04 \times 10^{-4} rsh \cos^2 \phi - 2.05 \times 10^{-5} rsh^2 \cos \phi - 0.677 \cos^3 \phi + 8.44 \times 10^{-8} rsh^3$ (-)	1.0000	
11.	$k_{T, Nov} = -4.89 \times 10^4 + 1.47 \times 10^5 \cos \phi - 3.20 \times 10^2 rsh + 6.40 \times 10^2 rsh \cos \phi - 1.47 \times 10^5 \cos^2 \phi$ $+ 1.42rsh^2 - 3.20 \times 10^2 rsh \cos^2 \phi - 1.42rsh^2 \cos \phi + 4.92 \times 10^4 \cos^3 \phi - 2.92 \times 10^{-3} rsh^3$ (-)	0.9999	
12.	$k_{T, Dec} = 0.506 - 1.25 \cos \phi + 0.521rsh - 2.80 \times 10^{-3} rsh \cos \phi + 1.52 \cos^2 \phi - 9.47 \times 10^{-6} rsh^2$ $+ 1.40 \times 10^{-3} rsh \cos^2 \phi + 9.50 \times 10^{-6} rsh^2 \cos \phi - 0.508 \cos^3 \phi - 1.06 \times 10^{-8} rsh^3$ (-)	1.0000	
13.	$k_{T, np} = -2.21 \times 10^5 + 6.62 \times 10^5 \cos \phi + 0.266rsh + 3.26 \times 10^2 rsh \cos \phi - 6.63 \times 10^5 \cos^2 \phi$ $- 2.75 \times 10^2 rsh^2 - 3.31 \times 10^{02} rsh \cos^2 \phi + 2.83 \times 10^{02} rsh^2 \cos \phi + 2.21 \times 10^{05} \cos^3 \phi - 4.52rsh^3$ (-)	0.9952	

Table 3. Eastern Region (periodic and non-periodic) models

S#	Model	R^2 (COD)	Model type
1.	$k_{T, Jan} = 0.715 - 1.88\cos\phi + 0.519rsh + 2.47 \times 10^{-3}rsh\cos\phi + 2.15\cos^2\phi + 1.77 \times 10^{-6}rsh^2 - 1.23 \times 10^{-3}rsh\cos^2\phi - 1.79 \times 10^{-6}rsh^2\cos\phi - 0.715\cos^3\phi + 8.96 \times 10^{-9}rsh^3$ (-)	1.0000	Periodic (monthly) models
2.	$k_{T, Feb} = 0.672 - 1.74\cos\phi + 0.519rsh + 2.84 \times 10^{-3}rsh\cos\phi + 2.02\cos^2\phi + 4.90 \times 10^{-6}rsh^2 - 1.42 \times 10^{-3}rsh\cos^2\phi - 4.91 \times 10^{-6}rsh^2\cos\phi - 0.672\cos^3\phi + 1.10 \times 10^{-9}rsh^3$ (-)	1.0000	
3.	$k_{T, Mar} = 0.565 - 1.42\cos\phi + 0.518rsh + 4.86 \times 10^{-3}rsh\cos\phi + 1.69\cos^2\phi + 3.44 \times 10^{-6}rsh^2 - 2.43 \times 10^{-3}rsh\cos^2\phi - 3.44 \times 10^{-6}rsh^2\cos\phi - 0.564\cos^3\phi - 4.36 \times 10^{-10}rsh^3$ (-)	1.0000	
4.	$k_{T, Apr} = 0.415 - 0.970\cos\phi + 0.514rsh + 1.11 \times 10^{-2}rsh\cos\phi + 1.24\cos^2\phi + 7.68 \times 10^{-6}rsh^2 - 5.56 \times 10^{-3}rsh\cos^2\phi - 7.69 \times 10^{-6}rsh^2\cos\phi - 0.411\cos^3\phi + 2.17 \times 10^{-9}rsh^3$ (-)	1.0000	
5.	$k_{T, May} = 0.695 - 1.81\cos\phi + 0.514rsh + 1.12 \times 10^{-2}rsh\cos\phi + 2.08\cos^2\phi + 8.83 \times 10^{-6}rsh^2 - 5.59 \times 10^{-3}rsh\cos^2\phi - 8.83 \times 10^{-6}rsh^2\cos\phi - 0.692\cos^3\phi - 5.80 \times 10^{-9}rsh^3$ (-)	1.0000	
6.	$k_{T, Jun} = 0.698 - 1.82\cos\phi + 0.516rsh + 8.69 \times 10^{-3}rsh\cos\phi + 2.09\cos^2\phi - 1.32 \times 10^{-6}rsh^2 - 4.35 \times 10^{-3}rsh\cos^2\phi + 1.28 \times 10^{-6}rsh^2\cos\phi - 0.696\cos^3\phi + 1.80 \times 10^{-8}rsh^3$ (-)	1.0000	
7.	$k_{T, Jul} = 0.758 - 2.00\cos\phi + 0.516rsh + 8.34 \times 10^{-3}rsh\cos\phi + 2.27\cos^2\phi + 1.31 \times 10^{-5}rsh^2 - 4.16 \times 10^{-3}rsh\cos^2\phi - 1.31 \times 10^{-5}rsh^2\cos\phi - 0.756\cos^3\phi - 1.48 \times 10^{-8}rsh^3$ (-)	1.0000	
8.	$k_{T, Aug} = 0.765 - 2.03\cos\phi + 0.518rsh + 4.12 \times 10^{-3}rsh\cos\phi + 2.30\cos^2\phi - 8.41 \times 10^{-6}rsh^2 - 2.06 \times 10^{-3}rsh\cos^2\phi + 8.37 \times 10^{-6}rsh^2\cos\phi - 0.765\cos^3\phi + 2.25 \times 10^{-8}rsh^3$ (-)	1.0000	
9.	$k_{T, Sep} = 0.965 - 2.62\cos\phi + 0.516rsh + 7.99 \times 10^{-3}rsh\cos\phi + 2.89\cos^2\phi + 2.66 \times 10^{-5}rsh^2 - 3.98 \times 10^{-3}rsh\cos^2\phi - 2.66 \times 10^{-5}rsh^2\cos\phi - 0.963\cos^3\phi - 1.65 \times 10^{-8}rsh^3$ (-)	1.0000	
10.	$k_{T, Oct} = 0.941 - 2.55\cos\phi + 0.515rsh + 1.08 \times 10^{-2}rsh\cos\phi + 2.82\cos^2\phi + 1.54 \times 10^{-5}rsh^2 - 5.37 \times 10^{-3}rsh\cos^2\phi - 1.54 \times 10^{-5}rsh^2\cos\phi - 0.939\cos^3\phi - 4.17 \times 10^{-9}rsh^3$ (-)	1.0000	
11.	$k_{T, Nov} = 0.888 - 2.39\cos\phi + 0.514rsh + 1.19 \times 10^{-2}rsh\cos\phi + 2.66\cos^2\phi + 1.01 \times 10^{-5}rsh^2 - 5.93 \times 10^{-3}rsh\cos^2\phi - 1.01 \times 10^{-5}rsh^2\cos\phi - 0.885\cos^3\phi - 1.25 \times 10^{-9}rsh^3$ (-)	1.0000	
12.	$k_{T, Dec} = 0.866 - 2.32\cos\phi + 0.516rsh + 7.03 \times 10^{-3}rsh\cos\phi + 2.59\cos^2\phi + 5.39 \times 10^{-6}rsh^2 - 3.51 \times 10^{-3}rsh\cos^2\phi - 5.40 \times 10^{-6}rsh^2\cos\phi - 0.864\cos^3\phi + 3.38 \times 10^{-9}rsh^3$ (-)	1.0000	
13.	$k_{T, np} = -3.70 \times 10^4 + 1.34 \times 10^5 \cos\phi - 17.3rsh - 1.25 \times 10^3 rsh\cos\phi - 1.57 \times 10^5 \cos^2\phi + 7.19 \times 10^2 rsh^2 + 1.34 \times 10^{03} rsh\cos^2\phi - 8.32 \times 10^{02} rsh^2\cos\phi + 5.96 \times 10^{04} \cos^3\phi + 62.7rsh^3$ (-)	0.9627	

Table 4. Central Region (periodic and non-periodic) models

S#	Model	R^2 (COD)	Model type
1.	$k_{T, Jan} = 5.22 \times 10^{02} - 1.04 \times 10^{03} \cos \phi - 4.34rsh + 4.86rsh \cos \phi + 5.19 \times 10^{02} \cos^2 \phi$ $+ 2.11 \times 10^{-04} rsh^2 \quad (-)$	0.9999	Periodic (monthly) models
2.	$k_{T, Feb} = 3.03 - 8.82 \cos \phi + 0.51905rsh + 1.88 \times 10^{-3} rsh \cos \phi + 9.09 \cos^2 \phi + 9.43 \times 10^{-6} rsh^2$ $- 9.36 \times 10^{-4} rsh \cos^2 \phi - 9.43 \times 10^{-06} rsh^2 \cos \phi - 3.03 \cos^3 \phi + 8.49 \times 10^{-10} rsh^3 \quad (-)$	1.0000	
3.	$k_{T, Mar} = 2.33 - 6.71 \cos \phi + 0.52075rsh - 1.52 \times 10^{-3} rsh \cos \phi + 6.98 \cos^2 \phi + 1.05 \times 10^{-5} rsh^2$ $+ 7.65 \times 10^{-4} rsh \cos^2 \phi - 1.05 \times 10^{-05} rsh^2 \cos \phi - 2.33 \cos^3 \phi + 2.88 \times 10^{-10} rsh^3 \quad (-)$	1.0000	
4.	$k_{T, Apr} = 2.71 - 7.84 \cos \phi + 0.52097rsh - 1.95 \times 10^{-3} rsh \cos \phi + 8.12 \cos^2 \phi + 6.48 \times 10^{-6} rsh^2$ $+ 9.81 \times 10^{-04} rsh \cos^2 \phi - 6.48 \times 10^{-06} rsh^2 \cos \phi - 2.71 \cos^3 \phi - 2.34 \times 10^{-09} rsh^3 \quad (-)$	1.0000	
5.	$k_{T, May} = 5.29 - 15.6 \cos \phi + 0.51483rsh + 1.03 \times 10^{-2} rsh \cos \phi + 15.9 \cos^2 \phi + 6.09 \times 10^{-6} rsh^2$ $- 5.16 \times 10^{-03} rsh \cos^2 \phi - 6.09 \times 10^{-06} rsh^2 \cos \phi - 5.29 \cos^3 \phi - 3.53 \times 10^{-10} rsh^3 \quad (-)$	1.0000	
6.	$k_{T, Jun} = 3.66 - 10.7 \cos \phi + 0.52089rsh - 1.76 \times 10^{-03} rsh \cos \phi + 11.0 \cos^2 \phi - 1.03 \times 10^{-05} rsh^2$ $+ 8.76 \times 10^{-04} rsh \cos^2 \phi + 1.03 \times 10^{-05} rsh^2 \cos \phi - 3.66 \cos^3 \phi - 1.99 \times 10^{-09} rsh^3 \quad (-)$	1.0000	
7.	$k_{T, Jul} = 4.29 - 12.6 \cos \phi + 0.52172rsh - 3.42 \times 10^{-03} rsh \cos \phi + 12.9 \cos^2 \phi - 8.12 \times 10^{-06} rsh^2$ $+ 1.71 \times 10^{-03} rsh \cos^2 \phi + 8.12 \times 10^{-06} rsh^2 \cos \phi - 4.29 \cos^3 \phi + 2.39 \times 10^{-09} rsh^3 \quad (-)$	1.0000	
8.	$k_{T, Aug} = 1.85 - 5.30 \cos \phi + 0.52998rsh - 2.00 \times 10^{-02} rsh \cos \phi + 5.57 \cos^2 \phi + 6.77 \times 10^{-07} rsh^2$ $+ 9.99 \times 10^{-03} rsh \cos^2 \phi - 6.72 \times 10^{-07} rsh^2 \cos \phi - 1.86 \cos^3 \phi - 2.36 \times 10^{-09} rsh^3 \quad (-)$	1.0000	
9.	$k_{T, Sep} = 0.696 - 1.82 \cos \phi + 0.52635rsh - 1.27 \times 10^{-02} rsh \cos \phi + 2.09 \cos^2 \phi + 7.01 \times 10^{-06} rsh^2$ $+ 6.36 \times 10^{-03} rsh \cos^2 \phi - 7.01 \times 10^{-06} rsh^2 \cos \phi - 0.699 \cos^3 \phi - 7.08 \times 10^{-10} rsh^3 \quad (-)$	1.0000	
10.	$k_{T, Oct} = -2.76 + 8.56 \cos \phi + 0.53256rsh - 2.51 \times 10^{-02} rsh \cos \phi - 8.28 \cos^2 \phi + 4.93 \times 10^{-06} rsh^2$ $+ 1.26 \times 10^{-02} rsh \cos^2 \phi - 4.93 \times 10^{-06} rsh^2 \cos \phi + 2.76 \cos^3 \phi - 3.26 \times 10^{-09} rsh^3 \quad (-)$	1.0000	
11.	$k_{T, Nov} = 1.72 - 4.89 \cos \phi + 0.52109rsh - 2.18 \times 10^{-03} rsh \cos \phi + 5.16 \cos^2 \phi + 8.39 \times 10^{-06} rsh^2$ $+ 1.10 \times 10^{-03} rsh \cos^2 \phi - 8.39 \times 10^{-06} rsh^2 \cos \phi - 1.72 \cos^3 \phi - 1.40 \times 10^{-09} rsh^3 \quad (-)$	1.0000	
12.	$k_{T, Dec} = 5.95 - 17.6 \cos \phi + 0.51341rsh + 1.32 \times 10^{-02} rsh \cos \phi + 17.9 \cos^2 \phi + 1.01 \times 10^{-05} rsh^2$ $- 6.58 \times 10^{-03} rsh \cos^2 \phi - 1.01 \times 10^{-05} rsh^2 \cos \phi - 5.95 \cos^3 \phi - 1.43 \times 10^{-09} rsh^3 \quad (-)$	1.0000	
13.	$k_{T, np} = -1.43 \times 10^4 + 4.24 \times 10^4 \cos \phi + 3.27 \times 10^{-3} rsh + 2.51 \times 10^{02} rsh \cos \phi - 4.18 \times 10^{04} \cos^2 \phi$ $- 2.24 \times 10^{02} rsh^2 - 2.51 \times 10^{02} rsh \cos^2 \phi + 2.24 \times 10^{02} rsh^2 \cos \phi + 1.38 \times 10^{04} \cos^3 \phi - 0.275 rsh^3 \quad (-)$	0.9998	

Table 5. Western Region (periodic and non-periodic) models

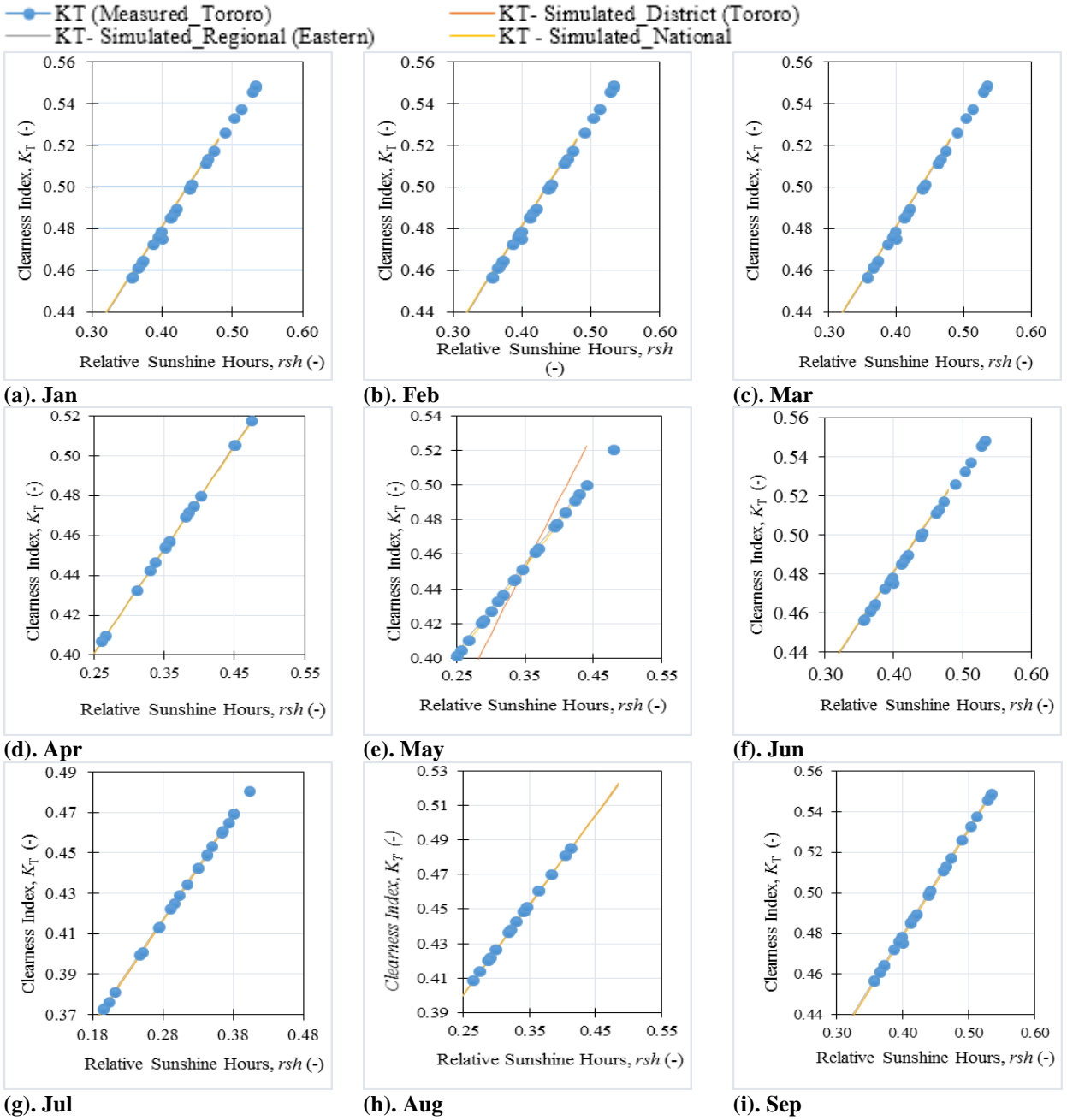
S#	Model	R^2 (COD)	Model type
1.	$k_{T, Jan} = 7.01 \times 10^{02} - 1.40 \times 10^{03} \cos \phi - 0.496rsh + 1.02rsh \cos \phi + 7.01 \times 10^{02} \cos^2 \phi - 1.26 \times 10^{-03} rsh^2 (-)$	0.9999	Periodic (monthly) models
2.	$k_{T, Feb} = 1.68 \times 10^{02} - 3.37 \times 10^{02} \cos \phi + 0.381rsh + 0.139rsh \cos \phi + 1.68 \times 10^{02} \cos^2 \phi + 2.64 \times 10^{-05} rsh^2 (-)$	0.9999	
3.	$k_{T, Mar} = 1.60136 - 4.53317 \cos \phi + 0.51741rsh + 5.18 \times 10^{-3} rsh \cos \phi + 4.80366 \cos^2 \phi + 5.51 \times 10^{-6} rsh^2 - 2.59 \times 10^{-3} rsh \cos^2 \phi - 5.50 \times 10^{-06} rsh^2 \cos \phi - 1.60115 \cos^3 \phi - 1.03 \times 10^{-08} rsh^3 (-)$	1.0000	
4.	$k_{T, Apr} = 1.49245 - 4.20687 \cos \phi + 0.51834rsh + 3.32 \times 10^{-3} rsh \cos \phi + 4.47779 \cos^2 \phi - 2.25 \times 10^{-7} rsh^2 - 1.66 \times 10^{-3} rsh \cos^2 \phi + 2.25 \times 10^{-7} rsh^2 \cos \phi - 1.49267 \cos^3 \phi - 9.31 \times 10^{-12} rsh^3 (-)$	1.0000	
5.	$k_{T, May} = 1.31588 - 3.67743 \cos \phi + 0.51912rsh + 1.76 \times 10^{-3} rsh \cos \phi + 3.94861 \cos^2 \phi - 2.73 \times 10^{-6} rsh^2 - 8.82 \times 10^{-4} rsh \cos^2 \phi + 2.73 \times 10^{-6} rsh^2 \cos \phi - 1.31636 \cos^3 \phi - 7.58 \times 10^{-11} rsh^3 (-)$	1.0000	
6.	$k_{T, Jun} = 1.16882 - 3.23688 \cos \phi + 0.52067rsh - 1.34 \times 10^{-3} rsh \cos \phi + 3.50871 \cos^2 \phi + 4.54 \times 10^{-7} rsh^2 + 6.71 \times 10^{-4} rsh \cos^2 \phi - 4.54 \times 10^{-7} rsh^2 \cos \phi - 1.16995 \cos^3 \phi - 1.14 \times 10^{-13} rsh^3 (-)$	1.0000	
7.	$k_{T, Jul} = 1.18346 - 3.28203 \cos \phi + 0.52303rsh - 6.06 \times 10^{-03} rsh \cos \phi + 3.55508 \cos^2 \phi - 4.67 \times 10^{-07} rsh^2 + 3.03 \times 10^{-03} rsh \cos^2 \phi + 4.60 \times 10^{-07} rsh^2 \cos \phi - 1.18581 \cos^3 \phi + 4.02 \times 10^{-09} rsh^3 (-)$	1.0000	
8.	$k_{T, Aug} = 1.00363 - 2.74235 \cos \phi + 0.52317rsh - 6.34 \times 10^{-03} rsh \cos \phi + 3.01522 \cos^2 \phi + 3.18 \times 10^{-06} rsh^2 + 3.17 \times 10^{-03} rsh \cos^2 \phi - 3.21 \times 10^{-06} rsh^2 \cos \phi - 1.0058 \cos^3 \phi + 1.73 \times 10^{-08} rsh^3 (-)$	1.0000	
9.	$k_{T, Sep} = 1.09081 - 3.00301 \cos \phi + 0.52114rsh - 2.28 \times 10^{-3} rsh \cos \phi + 3.27499 \cos^2 \phi + 2.30 \times 10^{-6} rsh^2 + 1.14 \times 10^{-3} rsh \cos^2 \phi - 2.30 \times 10^{-6} rsh^2 \cos \phi - 1.09209 \times 10^2 \cos^3 \phi - 4.43 \times 10^{-14} rsh^3 (-)$	1.0000	
10.	$k_{T, Oct} = 1.04353 - 2.86136 \cos \phi + 0.52169rsh - 3.38 \times 10^{-3} rsh \cos \phi + 3.13354 \cos^2 \phi + 1.61 \times 10^{-6} rsh^2 + 1.69 \times 10^{-3} rsh \cos^2 \phi - 1.61 \times 10^{-6} rsh^2 \cos \phi - 1.04501 \cos^3 \phi - 2.16 \times 10^{-13} rsh^3 (-)$	1.0000	
11.	$k_{T, Nov} = 4.12 \times 10^{-02} + 2.30 \times 10^{-02} \cos \phi + 5.20 \times 10^{-01} rsh (-)$	0.9999	
12.	$k_{T, Dec} = 1.81958 - 5.18823 \cos \phi + 0.5177rsh + 4.59 \times 10^{-3} rsh \cos \phi + 5.4591 \cos^2 \phi + 1.38 \times 10^{-6} rsh^2 - 2.30 \times 10^{-3} rsh \cos^2 \phi - 1.38 \times 10^{-06} rsh^2 \cos \phi - 1.81976 \cos^3 \phi + 9.11 \times 10^{-11} rsh^3 (-)$	1.0000	
13.	$k_{T, np} = 2.23 - 1.95 \cos \phi + 5.02 \times 10^{-01} rsh (-)$	0.9996	

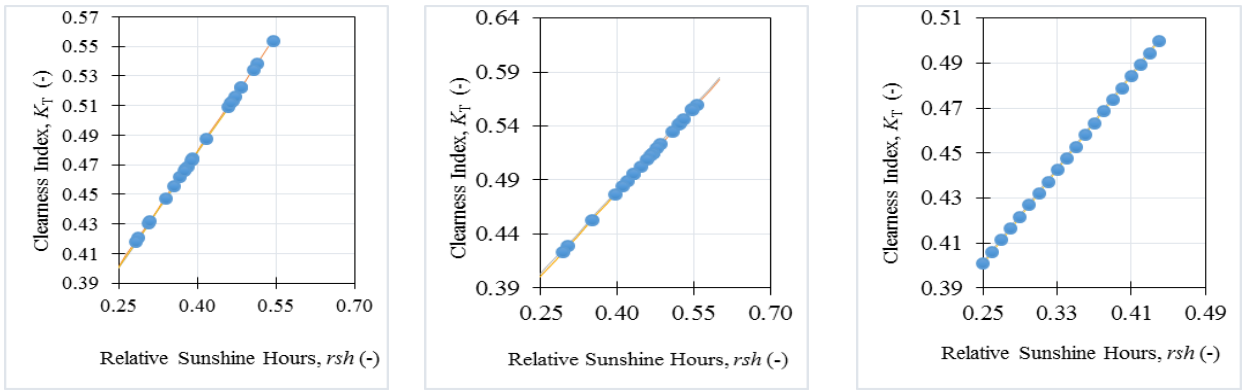
Table 6. Tororo District (periodic and non-periodic) models

S#	Model	R ² (COD)	Model type
1.	$k_{T, Jan} = 6.57 \times 10^{-02} + 7.29 \times 10^{-02} \cos \phi - 8.30 \times 10^{-03} rsh + 0.227 rsh \cos \phi + 6.08 \times 10^{-02} \cos^2 \phi - 0.138 rsh^2 + 0.302 rsh \cos^2 \phi + 0.138 rsh^2 \cos \phi + 7.13 \times 10^{-02} \cos^3 \phi + a_9 \times 10^{02} rsh^3$ (-)	1.0000	Periodic (monthly) models
2.	$k_{T, Feb} = 5.29 \times 10^{-02} + 0.106 \cos \phi + 0.283 rsh - 5.99 \times 10^{-02} rsh \cos \phi + 1.74 \times 10^{-02} \cos^2 \phi - 8.02 \times 10^{-02} rsh^2 + 0.297 rsh \cos^2 \phi + 8.02 \times 10^{-02} rsh^2 \cos \phi + 9.43 \times 10^{-02} \cos^3 \phi - 4.21 \times 10^{-12} rsh^3$ (-)	1.0000	
3.	$k_{T, Mar} = 7.71 \times 10^{-02} + 4.31 \times 10^{-02} \cos \phi - 0.240 rsh + 0.161 rsh \cos \phi + 9.98 \times 10^{-02} \cos^2 \phi - 5.25 \times 10^{-02} rsh^2 + 0.599 rsh \cos^2 \phi + 5.25 \times 10^{-02} rsh^2 \cos \phi + 5.07 \times 10^{-02} \cos^3 \phi + 3.22 \times 10^{-12} rsh^3$ (-)	1.0000	
4.	$k_{T, Apr} = 0.195 + 0.0753 \cos \phi + 0.520 rsh$ (-)	1.0000	
5.	$k_{T, May} = 9.22 \times 10^{-02} + 3.98 \times 10^{-03} \cos \phi + 9.76 \times 10^{-02} rsh + 0.180 rsh \cos \phi + 0.151 \cos^2 \phi + 0.284 rsh^2 + 0.242 rsh \cos^2 \phi - 0.284 rsh^2 \cos \phi + 2.35 \times 10^{-02} \cos^3 \phi - 2.06 \times 10^{-12} rsh^3$ (-)	1.0000	
6.	$k_{T, Jun} = 7.60 \times 10^{-02} + 4.61 \times 10^{-02} \cos \phi - 0.121 rsh + 0.275 rsh \cos \phi + 9.59 \times 10^{-02} \cos^2 \phi + 0.268 rsh^2 + 0.366 rsh \cos^2 \phi - 0.268 rsh^2 \cos \phi + a_8 \times 10^{05} \cos^3 \phi + a_9 \times 10^{02} rsh^3$ (-)	1.0000	
7.	$k_{T, Jul} = 7.93 \times 10^{-02} + 3.76 \times 10^{-02} \cos \phi + 0.460 rsh + 0.226 rsh \cos \phi + 0.107 \cos^2 \phi - 0.103 rsh^2 - 0.166 rsh \cos^2 \phi + 0.103 rsh^2 \cos \phi + 4.69 \times 10^{-02} \cos^3 \phi + 2.21 \times 10^{-12} rsh^3$ (-)	1.0000	
8.	$k_{T, Aug} = 5.72 \times 10^{-02} + 9.49 \times 10^{-02} \cos \phi - 5.44 \times 10^{-02} rsh + 0.536 rsh \cos \phi + 3.20 \times 10^{-02} \cos^2 \phi - 0.424 rsh^2 + 3.85 \times 10^{-02} rsh \cos^2 \phi + 0.424 rsh^2 \cos \phi + 8.66 \times 10^{-02} \cos^3 \phi - 4.59 \times 10^{-12} rsh^3$ (-)	1.0000	
9.	$k_{T, Sep} = 0.308 - 0.0374 \cos \phi + 0.520 rsh$ (-)	1.0000	
10.	$k_{T, Oct} = 8.65 \times 10^{-02} + 1.89 \times 10^{-02} \cos \phi + 0.124 rsh + 0.295 rsh \cos \phi + 0.132 \cos^2 \phi + 0.449 rsh^2 + 0.101 rsh \cos^2 \phi - 0.449 rsh^2 \cos \phi + 3.39 \times 10^{-02} \cos^3 \phi - 4.37 \times 10^{-13} rsh^3$ (-)	1.0000	
11.	$k_{T, Nov} = 5.19 \times 10^{-2} + 0.109 \cos \phi + 0.684 rsh - 0.118 rsh \cos \phi + 1.40 \times 10^{-2} \cos^2 \phi + 9.57 \times 10^{-2} rsh^2 - 4.63 \times 10^{-02} rsh \cos^2 \phi - 9.57 \times 10^{-02} rsh^2 \cos \phi + 9.61 \times 10^{-02} \cos^3 \phi - 1.06 \times 10^{-12} rsh^3$ (-)	1.0000	
12.	$k_{T, Dec} = 8.44 \times 10^{-5} + 2.44 \times 10^{-2} \cos \phi + 0.322 rsh + 0.173 rsh \cos \phi + 0.124 \cos^2 \phi - 4.02 \times 10^{-2} rsh^2 + 2.46 \times 10^{-2} rsh \cos^2 \phi + 4.02 \times 10^{-02} rsh^2 \cos \phi + 3.77 \times 10^{-2} \cos^3 \phi - 2.50 \times 10^{-12} rsh^3$ (-)	1.0000	
13.	$k_{T, np} = 8.40 \times 10^{-02} + 2.54 \times 10^{-02} \cos \phi + 0.636 rsh - 0.672 rsh \cos \phi + 0.123 \cos^2 \phi + 0.294 rsh^2 + 0.556 rsh \cos^2 \phi - 0.294 rsh^2 \cos \phi + 3.84 \times 10^{-02} \cos^3 \phi - 1.22 \times 10^{-10} rsh^3$ (-)	1.0000	

Table 7. Mbarara District (periodic and non-periodic) models

S#	Model	R^2 (COD)	Model type
1.	$k_{T, Jan} = 2.23 - 1.95 \cos \phi + 0.502rsh \quad (-)$	0.9872	Periodic (monthly) models
2.	$k_{T, Feb} = -8.37 \times 10^{-3} + 9.31 \times 10^{-2} \cos \phi + 2.65 \times 10^{-2} rsh + 0.238rsh \cos \phi - 0.211 \cos^2 \phi - 0.166rsh^2$ $+ 0.256rsh \cos^2 \phi + 1.66 \times 10^{-1} rsh^2 \cos \phi + 3.97 \times 10^{-1} \cos^3 \phi - 1.61 \times 10^{-12} rsh^3 \quad (-)$	1.0000	
3.	$k_{T, Mar} = -0.16 - 0.12 \cos \phi + 0.388rsh + 0.714rsh \cos \phi - 0.239 \cos^2 \phi - 0.211rsh^2$ $+ 0.821rsh \cos^2 \phi + 0.211rsh^2 \cos \phi - 1.80 \times 10^{-3} \cos^3 \phi - 3.96 \times 10^{-11} rsh^3 \quad (-)$	1.0000	
4.	$k_{T, Apr} = 0.122 + 4.97 \times 10^{-2} \cos \phi + 0.178rsh + 0.132rsh \cos \phi + 0.268 \cos^2 \phi - 0.150rsh^2$ $+ 0.210rsh \cos^2 \phi + 0.150rsh^2 \cos \phi - 0.169 \cos^3 \phi + 5.93 \times 10^{-12} rsh^3 \quad (-)$	1.0000	
5.	$k_{T, May} = 0.271 + 3.45 \times 10^{-3} \cos \phi + 0.143rsh + 0.0191rsh \cos \phi + 0.812 \cos^2 \phi + 0.0175rsh^2$ $+ 0.358rsh \cos^2 \phi - 1.75 \times 10^{-2} rsh^2 \cos \phi - 0.815 \cos^3 \phi + 5.63 \times 10^{-12} rsh^3 \quad (-)$	1.0000	
6.	$k_{T, Jun} = 0.063 + 0.069 \cos \phi + 0.165rsh + 0.486rsh \cos \phi + 0.052 \cos^2 \phi + 4.39 \times 10^{-3} rsh^2$ $- 0.130rsh \cos^2 \phi - 4.39 \times 10^{-3} rsh^2 \cos \phi + 0.0867 \cos^3 \phi + 6.96 \times 10^{-12} rsh^3 \quad (-)$	1.0000	
7.	$k_{T, Jul} = 9.48 \times 10^{-2} + 5.85 \times 10^{-2} \cos \phi + 1.29 \times 10^{-2} rsh + 0.125rsh \cos \phi + 0.168 \cos^2 \phi - 0.239rsh^2$ $+ 0.382rsh \cos^2 \phi + 0.239rsh^2 \cos \phi - 5.02 \times 10^{-2} \cos^3 \phi + 5.37 \times 10^{-12} rsh^3 \quad (-)$	1.0000	
8.	$k_{T, Aug} = 3.74 \times 10^{-2} + 7.79 \times 10^{-2} \cos \phi - 1.84 \times 10^{-2} rsh + 0.354rsh \cos \phi - 4.34 \times 10^{-2} \cos^2 \phi - 0.0489rsh^2$ $+ 0.184rsh \cos^2 \phi + 0.0489rsh^2 \cos \phi + 1.99 \times 10^{-2} \cos^3 \phi - 2.21 \times 10^{-12} rsh^3 \quad (-)$	1.0000	
9.	$k_{T, Sep} = 3.83 \times 10^{-2} + 7.74 \times 10^{-2} \cos \phi + 0.148rsh + 0.350rsh \cos \phi - 4.01 \times 10^{-2} \cos^2 \phi + 0.201rsh^2$ $+ 2.20 \times 10^{-2} rsh \cos^2 \phi - 0.201rsh^2 \cos \phi + 0.195 \cos^3 \phi - 2.11 \times 10^{-12} rsh^3 \quad (-)$	1.0000	
10.	$k_{T, Oct} = 9.93 \times 10^{-2} + 5.73 \times 10^{-2} \cos \phi + 0.533rsh - 2.06 \times 10^{-2} rsh \cos \phi + 0.183 \cos^2 \phi + 0.534rsh^2$ $+ 8.14 \times 10^{-3} rsh \cos^2 \phi - 0.534rsh^2 \cos \phi - 0.9687 \cos^3 \phi + 7.38 \times 10^{-12} rsh^3 \quad (-)$	1.0000	
11.	$k_{T, Nov} = 8.18 \times 10^{-2} + 6.30 \times 10^{-2} \cos \phi + 0.599rsh + 1.89 \times 10^{-2} rsh \cos \phi + 0.119 \cos^2 \phi - 0.183rsh^2$ $- 0.0974rsh \cos^2 \phi + 0.0183rsh^2 \cos \phi + 6.67 \times 10^{-3} \cos^3 \phi - 2.29 \times 10^{-13} rsh^3 \quad (-)$	1.0000	
12.	$k_{T, Dec} = 4.68 \times 10^{-2} + 7.47 \times 10^{-2} \cos \phi + 0.227rsh + 0.125rsh \cos \phi - 9.07 \times 10^{-3} \cos^2 \phi + 0.0257rsh^2$ $+ 0.168rsh \cos^2 \phi - 2.57 \times 10^{-2} rsh^2 \cos \phi + 0.158 \cos^3 \phi + 1.38 \times 10^{-12} rsh^3 \quad (-)$	1.0000	
13.	$k_{T, np} = 0.22 + 0.0511 \cos \phi + 0.52rsh \quad (-)$	1.0000	Non-periodic





(j). Oct (k). Nov (l). Dec
Figure 1. Periodic (monthly) validation of cleanness index for Tororo district

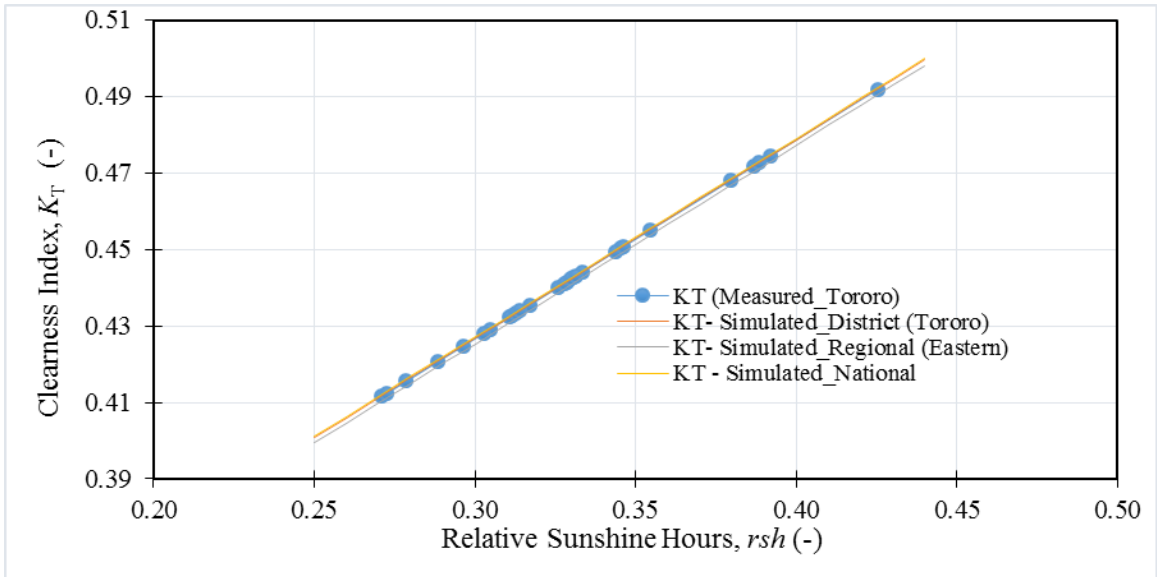
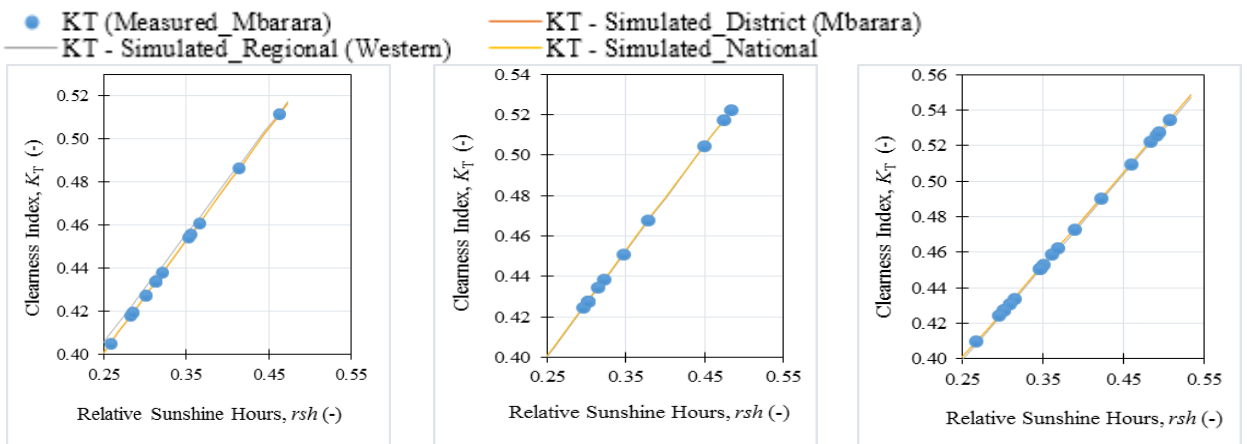


Figure 2. Non-periodic validation of cleanness index for Tororo district



(a). Jan (b). Feb (c). Mar

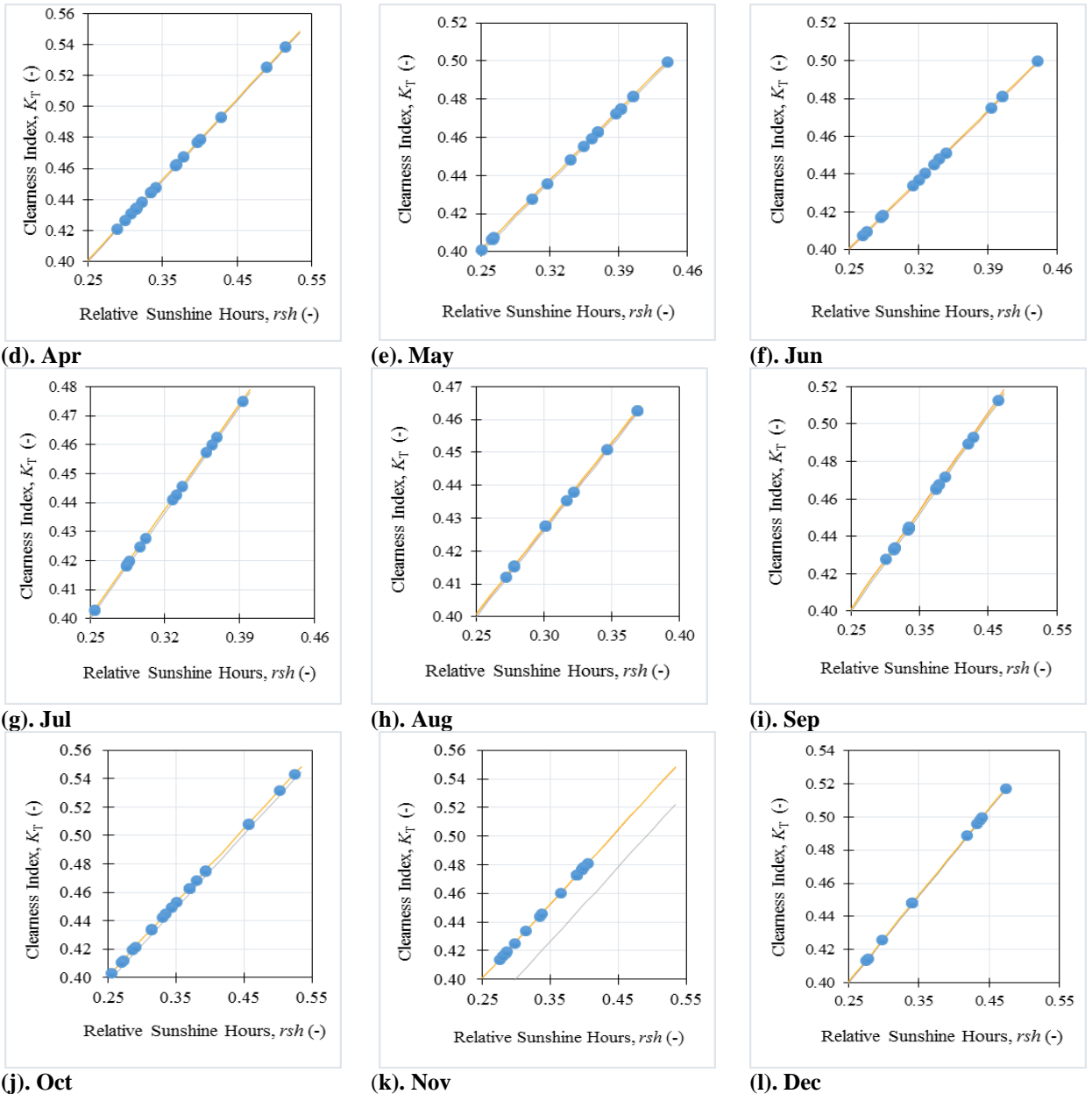


Figure 3. Periodic (monthly) validation of clearness index for Mbarara district

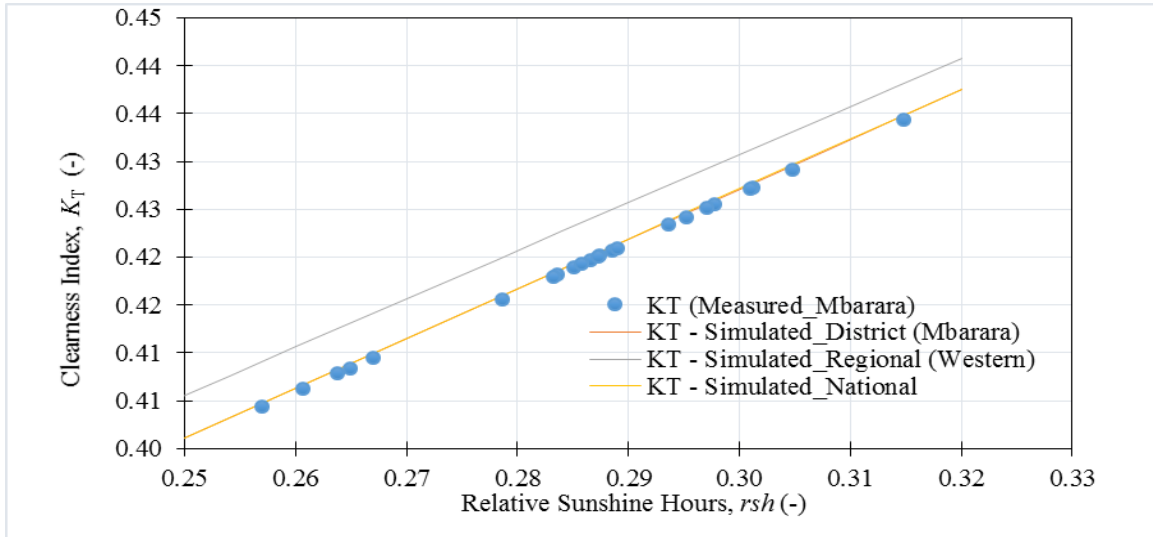


Figure 4. Non-periodic validation of clearness index for Mbarara district

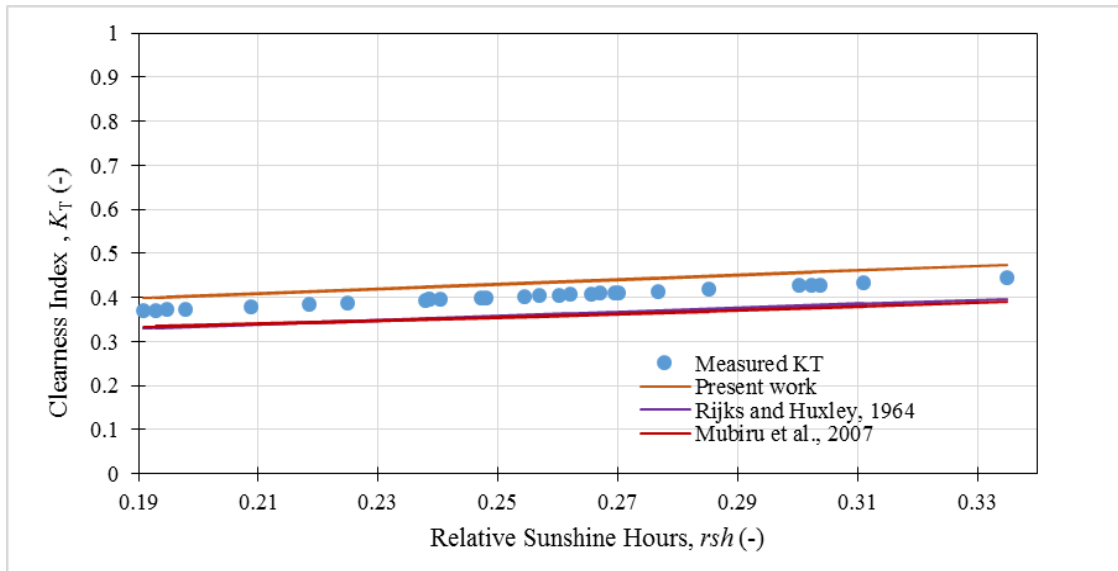


Figure 5. Comparison of Clearness Index Models in Uganda

There is much deception in the satellite tracked from the region. The difference in the region can be attributed to variation in topography of the Western region (which is mountainous in nature) whereas the deviation in Tororo district could be impacted by the peculiar latitude and longitude of the district which is an obvious problem associated with the satellite data [22].

Considering Figures 2 and 4, Figure 2 validated well for non-periodic models at all levels authenticating cohesion in the satellite and measured data. Whereas, Figure 4, shows an irregular behavior by deviating far from locally measured meteorological data. This shows that there is discrepancy in the measured and satellite data. Where there are cases of absolute deviations between satellite and the meteorological data could be attributed to failure to proper calibration, otherwise, this study has shown there is conformity in both measured and satellite data. Thus, NASA data has been confirmed to be consistent with on-station data in Uganda and could be used elsewhere (in other countries).

To authenticate the validity of the present work with existing models ([12] and [13]), the present work fitted with the meteorological data more than the existing ones as portrayed in Figure 5. However, the present work laid over the meteorological data with smaller deviation compared to the existing models which is below the meteorological data with wider deviation. The present model is encompassing because it covers all the regions (4), districts (122) and few validated district (2) of Uganda. Thus, the present model is recommended for computing clearness index and global solar radiation for Uganda.

4.0 Conclusions

This study has carried out comprehensive model on climatological parameter (clearness index) for all geographical locations of Uganda; Northern, Eastern, Central, Western with focus on all the districts (122) to develop a validated clearness index model, which is function of latitude of the locality and its relative sunshine hours to uncombined and combined variables physical model. It is observed

that clearness index ranges for different regions in Uganda: Northern region (0.5288 - 0.6077), Eastern (0.5609 - 0.6077), Central (0.5123 - 0.6224) and Western (0.5123 - 0.5893) regions. District wise could be furnished by the models on the specifications of latitude and relative sunshine hours on monthly or yearly basis. There was remarkable agreement between the satellite and measured data indicating that the national meteorological centers are consistent in calibration the equipment and also NASA data is efficient in carrying out climatological investigations for computing three monthly average terrestrial power on a horizontal surface. The present study has found that seldom deviation in the clearness index is attributed to impact of latitude and longitude of the location of the locality. This study is strongly recommending the clearness index models for estimating clearness index and for computing power potential in Uganda. It could be useful for modelling global solar radiation and for validating existing global solar radiation model, and wider applications in solar engineering in Uganda.

Acknowledgements

The authors do acknowledge; the Department of Physics, Makerere University (Uganda), for the provision of meteorological data and NASA POWER for availing the data used in the development and analysis of the clearness index in Uganda.

Conflict of Interests

The authors wish to declare that there is no conflict of interest in the work.

Declaration of Funding

The authors wish to declare that there is no funding for this work

Nomenclature

sh	Sunshine hours
sh_{av}	Average sunshine hours
rsh	Relative sunshine hours
rsh_{av}	Average relative sunshine hours
ϕ	Latitude

ΔT	Change in temperature
T_{av}	Average temperature
H	Humidity
H_{av}	Average humidity
RH	Relative humidity

References

1. Bayrakçı, H.C., C. Demircan, and A. Keçebaş, *The development of empirical models for estimating global solar radiation on horizontal surface: A case study*. Renewable and Sustainable Energy Reviews, 2018. **81**: p. 2771-2782.
2. Mbiaké, R., et al., *The Relationship between Global Solar Radiation and Sunshine Durations in Cameroon*. Open Journal of Air Pollution, 2018. **7**(2): p. 107-119.
3. Soulouknga, M.H., et al., *Evaluation of global solar radiation from meteorological data in the Sahelian zone of Chad*. Renewables: Wind, Water, and Solar, 2017. **4**(1): p. 4.
4. Onyango, A.O. and V. Ongoma, *Estimation of mean monthly global solar radiation using sunshine hours for Nairobi City, Kenya*. Journal of renewable and sustainable energy, 2015. **7**(5): p. 053105.
5. Agbo, G., A. Baba, and T. Obiekezie, *Empirical models for the correlation of monthly average global solar radiation with sunshine hours at Minna, Niger State, Nigeria*. Journal of Basic Physical Research, 2010. **1**(1): p. 41-47.
6. Augustine, C. and M. Nnabuchi, *Correlation between sunshine hours and global solar radiation in Warri, Nigeria*. Pacific Journal of Science and Technology, 2009. **10**(2): p. 574-579.
7. Ahmed, F. and I. Ulfat, *Empirical models for the correlation of monthly average daily global solar radiation with hours of sunshine on a horizontal surface at Karachi, Pakistan*. Turkish Journal of Physics, 2004. **28**(5): p. 301-307.
8. Nwokolo, S.C. and C.Q. Otse, *Impact of Sunshine Duration and Clearness Index on Diffuse Solar Radiation Estimation in Mountainous Climate*. Trends in Renewable Energy, 2019. **5**(3): p. 307-332.
9. Yusuf, A., *Characterization of sky conditions using clearness index and relative sunshine duration for Iseyin, Nigeria*. International Journal of Physical Sciences Research, 2017. **1**(1): p. 53-60.
10. Poudyal, K., et al., *Estimation of global solar radiation using sunshine duration in Himalaya Region*. Research Journal of chemical sciences, 2012. **2**(11): p. 20-25.
11. Suehrcke, H., R.S. Bowden, and K. Hollands, *Relationship between sunshine duration and solar radiation*. Solar Energy, 2013. **92**: p. 160-171.
12. Rijks, D. and P. Huxley, *The empirical relation between solar radiation and hours of bright sunshine near Kampala, Uganda*. Journal of Applied Ecology, 1964: p. 339-345.
13. Mubiru, J., et al., *Assessing the performance of global solar radiation empirical formulations in Kampala, Uganda*. Theoretical and Applied Climatology, 2007. **87**(1-4): p. 179-184.
14. Asilevi, P.J., et al., *Modeling the spatial distribution of Global Solar Radiation (GSR) over Ghana using the Ångström-Prescott sunshine duration model*. Scientific African, 2019. **4**: p. e00094.
15. Assi, A., M. Jama, and M. Al-Shamisi, *Prediction of global solar radiation in Abu Dhabi*. ISRN Renewable Energy, 2012. **2012**.
16. Ahwide, F., A. Spena, and A. El-Kafrawy, *Correlation for the average daily diffuse fraction with clearness index and estimation of beam solar radiation and possible sunshine hours fraction in Sabha, Ghadames and Tripoli-Libya*. APCBEE procedia, 2013. **5**: p. 208-220.
17. Muzathik, A., et al., *Daily Global Solar Radiation Estimate Based on Sunshine Hours*. International journal of mechanical and materials engineering, 2011. **6**(1): p. 75-80.
18. Matuszko, D., *Influence of cloudiness on sunshine duration*. International Journal of Climatology, 2012. **32**(10): p. 1527-1536.
19. Zhu, W., et al., *Estimating Sunshine Duration Using Hourly Total Cloud Amount Data from a Geostationary Meteorological Satellite*. Atmosphere, 2020. **11**(1): p. 26.
20. ALAM, F., et al., *Empirical model development for the estimation of clearness index using meteorological parameters*. Turkish Journal of Electrical Engineering &

- Computer Sciences, 2019. **27**(6): p. 4429-4441.
21. Mohandes, M.A. and S. Rehman, *Estimation of sunshine duration in Saudi Arabia*. Journal of Renewable and Sustainable Energy, 2013. **5**(3): p. 033128.
 22. NASA. *MY NASA DATA: Investigating Factors that Influence Climate*. 2020 [cited 2020 10th April 2020]; Available from: <https://science.nasa.gov/my-nasa-data-investigating-factors-influence-climate>.